Inhibition of itch by neurokinin 1 receptor (Tacr1) -expressing ON cells in the rostral ventromedial medulla

Authors: Taylor Follansbee[1,2], Dan Domocos[3], Eileen Nguyen[4], Amanda Nguyen[1], Aristea Bountouvas[1], Lauren Velasquez[1], Mirela Iodi Carstens[1], Keiko Takanami[5], Sarah E. Ross[4], E. Carstens[1]

[1]Department of Neurobiology, Physiology and Behavior, Univ. of California, Davis CA 95616, USA

[2]Department of Neuroscience, Johns Hopkins University, Baltimore MD 21205

[3]Department of Anatomy, Animal Physiology and Biophysics, University of Bucharest, Bucharest, Romania

[4]Pittsburgh Center for Pain Research and Department of Neurobiology, University of Pittsburgh, Pittsburgh, PA 15213, USA

[5]Dept. of Environmental Life Science, National Nara Women University, Nara Japan

Abstract

The rostral ventromedial medulla (RVM) is important in descending modulation of spinal nociceptive transmission, but it is unclear if the RVM also modulates spinal pruriceptive transmission. RVM ON cells are activated by noxious algesic and pruritic stimuli and are pronociceptive. Many RVM-spinal projection neurons express the neurokinin-1 receptor (Tacr1), and ON-cells are excited by local administration of substance P (SP). We hypothesized that Tacr1-expressing RVM ON cells exert an inhibitory effect on itch opposite to their pronociceptive action. Intramedullary microinjection of SP significantly potentiated RVM ON cells and reduced pruritogen-evoked scratching while producing mild mechanical sensitization. Chemogenetic activation of RVM Tacr1-expressing RVM neurons also reduced acute pruritogen-evoked scratching. Optotagging experiments confirmed RVM Tacr1-expressing neurons to be ON cells. We conclude that Tacr1-expressing ON cells in RVM play a significant role in the modulation of pruriceptive transmission.

Introduction

The transmission of somatosensory information in the spinal cord is under top-down modulation and has been extensively studied in the context of pain signaling. Descending modulation of pain is reflected by phenomena such as expectation (placebo and nocebo), diffuse noxious inhibitory control (DNIC) and conditioned pain modulation (CPM) (Bartels et al., 2018; Chebbi et al., 2014; Damien et al., 2018; Le Bars, 2002; Lockwood & Dickenson, 2020). Descending modulation is also thought to underlie stress mediated changes in pain threshold, with acute stress inhibiting and chronic stress facilitating nociceptive transmission (Butler & Finn, 2009; Fields, 2000; Jennings et al., 2014; Wager & Atlas, 2015). Recent studies indicate that the spinal transmission of pruriceptive information is also under descending modulatory influences, but it is not known whether itch is modulated in the same way as pain (Agostinelli & Bassuk, 2021; Gao et al., 2021; Gao et al., 2019; Koga et al., 2020; Liu et al., 2019; Samineni et al., 2019; Wu et al., 2021).

The rostral ventromedial medulla (RVM) contains neurons with descending projections to the spinal cord which bidirectionally modulate spinal nociceptive transmission (Fields, 2000; Fields & Basbaum, 1978; Fields & Heinricher, 1985; Heinricher et al., 2009; Millan, 2002; Ossipov et al., 2014). RVM ON cells are excited and OFF cells are inhibited by noxious stimulation just prior to a nocifensive withdrawal reflex, and respectively facilitate and inhibit spinal nociceptive transmission (Fields, 2004; Fields et al., 1983). Increased ON cell and decreased OFF cell firing are thought to contribute to the chronification of pain (Ossipov et al., 2014). Neutral cells do not exhibit any significant response to noxious stimulation (Barbaro et al., 1986). Many RVM neurons project to the spinal cord via the dorsolateral funiculus (DLF), terminating in layers I, II and V, and are implicated in the analgesic effects of opioids. It is still unknown whether the RVM ON and OFF cells are involved in the modulation of itch transmission.

A recent study reported that neurons in the periaqueductal gray (PAG) expressing Tac1, the gene for substance P (SP), project to and make an excitatory glutamatergic connection with neurons in the RVM (Gao et al., 2019). Activation of these PAG neurons promotes scratching. A population of GABAergic neurons originating in the RVM synapse onto spinal neurons that express the gastrin releasing peptide receptor (GRPR) (Liu et al., 2019), which are considered to be essential for spinal pruriceptive transmission (Carstens et al., 2020). Activation of GABAergic and inhibition of glutamatergic neurons in PAG reduced scratching behavior in both acute and chronic itch conditions (Samineni et al., 2019). Furthermore, pruritogens were shown to excite ON and inhibit OFF cells (Follansbee et al., 2018). Cervical cold block, which diminishes activity in descending modulatory pathways, decreased pruritogen-evoked activity and facilitated algogen-evoked activity of spinal cord neurons implying opposing effects of descending modulatory pathways on nociceptive and pruriceptive transmission (Carstens et al., 2018). The current evidence suggests that at least two classes of PAG neurons, via connections to RVM cells, exert bimodal effects on the spinal pain and itch signaling pathways. Since activation of PAG *tac1r* neurons facilitates itch this implies that activation of RVM Tacr1-expressing neurons may likewise facilitate itch. However, RVM ON cells are known to facilitate pain, and thus may have an opposing effect on itch transmission.

Here we investigated the role of Tacr1-expressing RVM neurons in itch modulation. In the present study, we used pharmacological and opto/chemogenetic methods to selectively activate RVM Tacr1-expressing cells, which we hypothesize represent a population of RVM ON cells, and assessed the effects on pruritogen-evoked scratching, and thermal and mechanical nociceptive behavior. When RVM Tacr1-expressings cells were activated we observed that itch related behaviors were inhibited, while producing mild mechanical sensitization. We used optotagging to characterize these RVM Tacr1-expressing neurons as RVM ON cells. These

78 results are the first to demonstrate an inhibitory effect of RVM ON cells on itch transmission,
79 contrary to their known pronociceptive function.

80 **Results**

81 SP enhances RVM ON-cell responses to pinch

82 In rats, responses of RVM ON cells were potentiated by intramedullary microinjection of the
83 Tacr1 agonist SP (Budai et al., 2007) and we wished to determine whether this is true in mouse.
84 We identified RVM ON cells using in vivo extracellular electrophysiological recordings, with the
85 criterion that noxious pinch elicited a > 30% increase in firing that preceded the onset of the
86 hindpaw withdrawal. Using a microinjection cannula attached to a recording microelectrode (Fig.
87 1A), SP or saline was microinjected while recording from an ON cell in anesthetized mice.

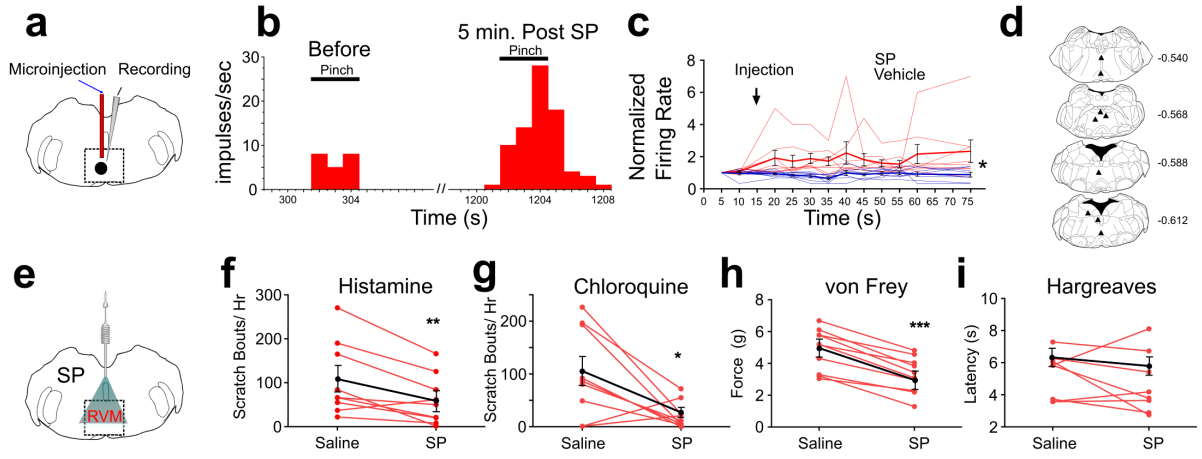

Figure 1: Effects of intramedullary microinjection of SP on RVM ON cells and itch and pain behavior. (A) SP or saline was microinjected while recording from single ON cells. (B) Peristimulus-time histogram of ON cell response to pinch before (left) and 5 min after local microinjection of SP (right). (C) Normalized firing rate of ON cells following local microinjection of saline (blue, n = 8) or SP (red, n = 8) at time indicated by arrow. ON cells showed a significant increase in evoked firing following SP injection compared with saline (*; p = 0.0133, 2-way ANOVA, bolded lines: mean responses; error bars SEM). Male mice were used in these experiments. (D) Lesion sites from the RVM ON cell recordings. Numbers to right indicate Bregma coordinates. (E) An implanted intramedullary microinjection cannula allowed assessment of itch and pain behavior after injection of SP into RVM. (F, G) Graphs plot the number of scratch bouts elicited by intradermal injection of histamine (F) or chloroquine (G) for each mouse (red dots and lines), and mean scratch bouts (black line; error bars: SEM), following intramedullary microinjection of saline or SP. Experiments with saline and SP microinjections were conducted at least 7 days apart. Microinjection of SP significantly attenuated histamine- and chloroquine-evoked scratching (F, G). (H) Mechanical withdrawal thresholds were reduced by intramedullary SP. (I) Thermal withdrawal latency was not significantly affected by intramedullary SP. *p < 0.05, **p < 0.01, ***p < 0.001. n = 5-7 males, 3 females/ group.

Microinjection of SP potentiated pinch-evoked responses (Fig.1B). Following SP microinjection, normalized responses of ON cells to repeated pinch stimuli were significantly increased (Fig. 1C). The enhancement of responses lasted > 1 hr. Histologically recovered recording sites were located within the RVM and adjacent regions of the medullary reticular formation (Fig. 1D). These results show that, similar to rats, RVM ON cells in the mouse are potentiated following localized injection of SP.

Intramedullary SP inhibits scratching

Since RVM ON cells are potentiated following injection of SP, we next tested if intramedullary microinjection of SP affected itch and pain related behaviors. Mice were implanted with an intramedullary microinjection cannula dorsal to the RVM to allow microinjection of SP or vehicle (Fig. 1E). The number of scratch bouts elicited by intradermal injection of histamine was significantly lower following intramedullary microinjection of SP compared to saline vehicle (Fig. 1F). Scratching elicited by intradermal injection of chloroquine was also significantly reduced following intramedullary injection of SP compared to saline (Fig. 1G).

There was a significant decrease in mechanical force to elicit a hindlimb withdrawal following intramedullary SP compared to vehicle injection (Fig. 1H), indicating mild mechanical sensitization. There was no significant effect of intramedullary SP injection on thermal hindpaw withdrawal latency (Fig. 1I). We observed that both male and female mice showed a reduced hindlimb withdrawal, but that males had a significantly higher force for both saline and sp injection when compared with females (Supplemental Fig. 6d). Thus, activation of RVM Tacr1-expressing neurons, through intramedullary injection of SP, resulted in facilitation of mechanical nociceptive behavior and inhibition of pruritogen-evoked scratching behavior.

Targeted expression of DREADDs in RVM Tacr1 expressing neurons

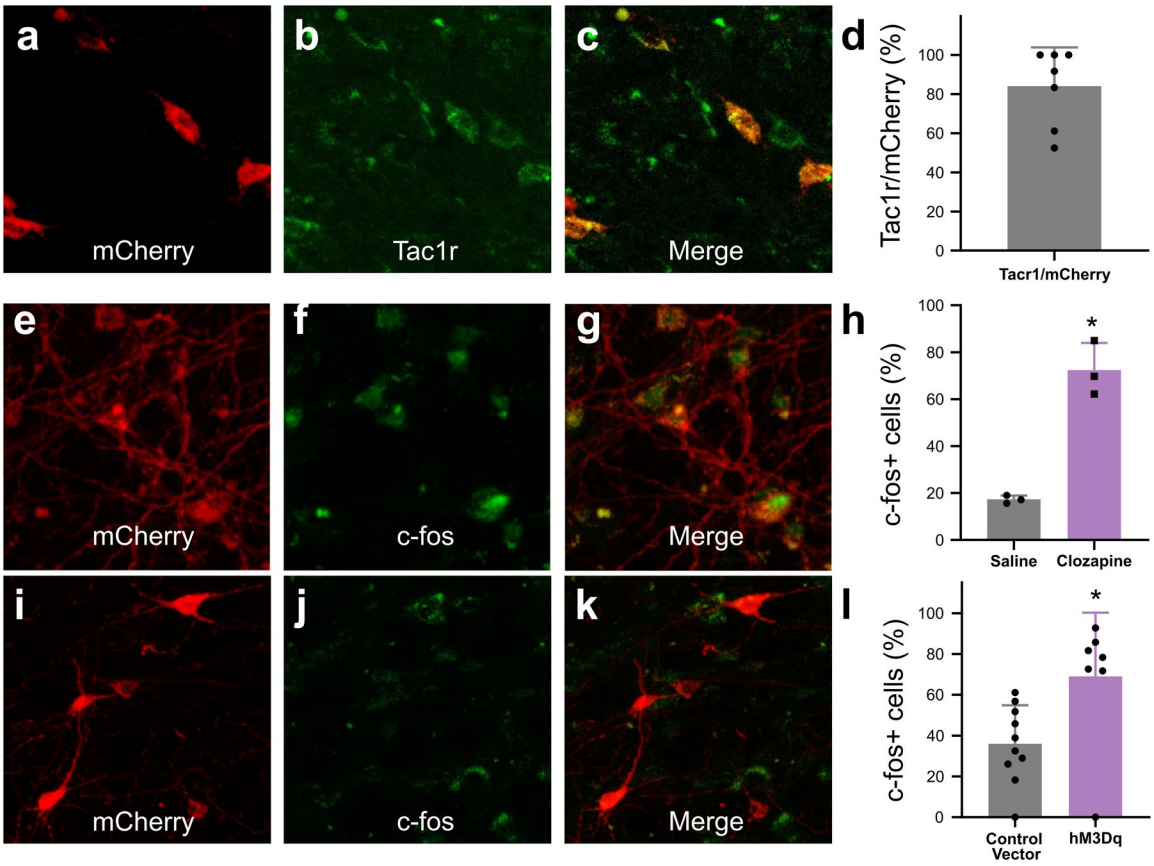

Figure 2: In Tacr1 cre $^{+/-}$ mice receiving AAV-DIO-hM3Dq-mCherry injections in the RVM, mCherry strongly colocalized with Tacr1 expression and clozapine strongly increased Tacr1 cellular activity. (A-C): images of RVM cells expressing mCherry (A), anti-Tacr1 antibody (B), and double-labeled cells (C). (D): 84% of cells exhibited co-localization of Tacr1 and mCherry. (E-G): images of RVM neurons expressing mCherry (E), c-fos (F) and double-labeled cells (G) after clozapine administration in mice that had received AAV-DIO-hM3Dq-mCherry injections in RVM. (H). In DREADDs mice, injection of clozapine significantly increased the number of c-fos+ neurons when compared with saline injection. (I-K): images of RVM neurons expressing mCherry (I), c-fos (J) and double-labeled cells (K) after clozapine administration in mice that had received AAV-DIO-mCherry injections in RVM. (L): Following administration of clozapine, the number for c-fos+ neurons was significantly greater when compared to vector controls. N = 3-10/group, *p < 0.05, unpaired students t test.

We next wanted to determine whether activation of RVM Tacr1 expressing neurons, would modulate itch related behaviors. To selectively target Tacr1-expressing neurons in the RVM we employed a chemogenetic approach. AAV-DIO-hM3dq-mCherry was injected into the RVM of Tacr1 cre mice, resulting in selective expression of hM3Dq in Tacr1-expressing neurons (84% expression of DREADDs in Tacr1 positive cells, Fig. 2A-C).

To activate the DREADDs (hM3Dq), clozapine was injected at a dose 0.01 mg/kg (Gomez et al., 2017). This dose of clozapine was sufficient to produce increased activity of DREADDs-

expressing neurons measured by c-fos expression. When we tested DREADDs mice there was a significant increase in the number of c-fos positive cells following ip administration of clozapine (62.22% +/- 11.61%) when compared with ip saline (15.66% +/- 1.678%) (Fig. 2h). In addition, we tested if clozapine elicited a greater increase in c-fos expression in DREADDs compared to control vector (mCherry) mice. Indeed, following clozapine administration, the number of c-fos positive mCherry-expressing cells was significantly higher in DREADDs (hM3Dq-mCherry) mice (68.98% +/- 11.83%) compared with neurons from control vector (mCherry) mice (36.02% +/- 5.96%; Fig. 3 I-L, p = 0.0158). These results show that injection of clozapine activates hM3Dq, which is expressed by RVM Tacr1 neurons.

Activation of RVM Tacr1 expressing neurons inhibits acute itch

To test the functional role of the RVM Tacr1-expressing population of neurons in itch modulation, we used DREADDs (hM3dq) to activate these neurons during pruritogen-evoked scratching behaviors. Activation of DREADD-expressing RVM neurons in Tacr1 cre mice using clozapine significantly attenuated pruritogen-evoked scratching behavior. After clozapine administration (0.01 mg/kg, ip) there was a significant reduction in scratch bouts elicited by intradermal histamine as compared to systemic administration of saline vehicle (Fig. 3C). There was a significantly stronger inhibition of histamine-evoked scratching behavior in male compared to female mice (Supplemental Fig. 6e). Similarly, there was a significant reduction in chloroquine-evoked scratching (Fig. 4D). In contrast, clozapine administration had no significant effect on the withdrawal threshold to mechanical von Frey stimuli (Fig. 4E) or withdrawal latency to thermal stimulation (Fig. 3F). Administration of clozapine in control vector (Tacr1-mCherry) mice had no significant effect on scratching behavior elicited by intradermal injection of histamine (Fig. 3C) or chloroquine (Fig. 3D). Likewise, clozapine administration had no significant effect on mechanical (Fig. 3E) or thermal hindpaw withdrawals in vector controls (Fig. 3F). Finally, neither a low (0.01 mg/kg) nor a higher dose (0.1 mg/kg) of clozapine had any

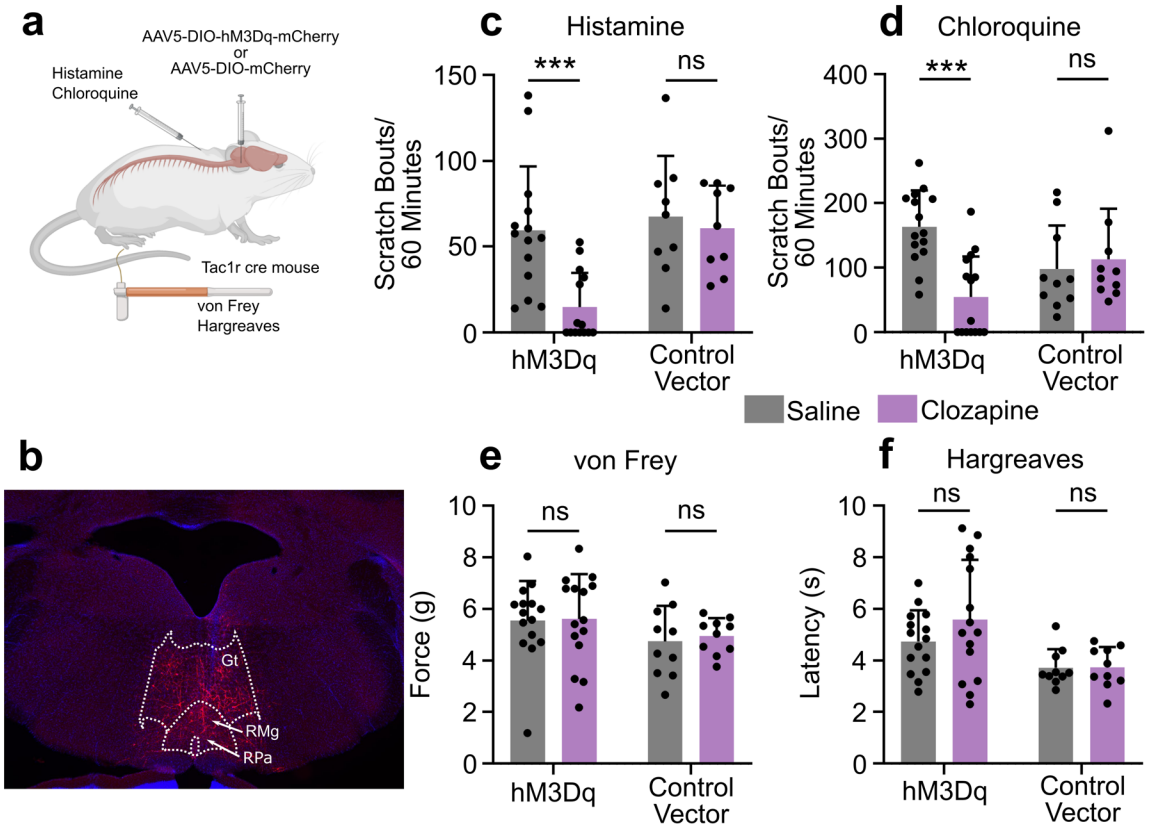

Figure 3: Chemogenetic activation of RVM Tacr1 expressing neurons inhibits itch related behavior. (A) AAV5-DIO-hM3Dq-mCherry or AAV5-DIO-mCherry was injected into the RVM of Tacr1 cre mice. (B) Expression of hM3Dq-mCherry was limited to the RVM. Gt: gigantocellularis; RMg: raphe magnus; RPa: raphe pallidus. (C) Administration of clozapine caused a significant reduction in histamine-evoked scratching (7 males, 7 females) in hM3Dq expressing mice, but not in control vector mice (6 males, 3 females). (D) Administration of caused a significant reduction in chloroquine-evoked scratching in hM3Dq mice (7 males, 8 females) but not in control vector mice (6 males, 4 females). (E) Clozapine administration did not significantly change mechanical withdrawal thresholds in hM3Dq (7 males, 8 females) or control vector mice (6 males, 4 females). (F) Clozapine administration did not significantly change thermal withdrawal thresholds in hM3Dq (7 males, 8 females) or control vector mice (6 males, 4 females). *p < 0.05, **p < 0.01, ***p < 0.001, Two-way ANOVA with Sidaks multiple comparison test.

significant effect on histamine- or chloroquine-evoked scratching behavior or on mechanically-

or thermally-evoked paw withdrawals in wildtype mice (Supplemental Fig. 2).

Our results were independently confirmed using a separate line of tac1Rcre-ER mice (Huang et al. 2016), that received intra-RVM microinjection of the excitatory DREADD AAV2-DIO-hM3dq-mCherry. Chemogenetic activation using CNO significantly reduced chloroquine evoked scratch bouts (Supplemental Fig. 1A) and spontaneous scratching behavior (Supplemental Fig. 1B), and also significantly reduced the von Frey mechanical withdrawal threshold (Supplemental

Fig. 1C) with no effect on thermal withdrawal latency (Supplemental Fig. 1D). CNO had no effect in the control vector mice. Independent experiments in two lines of Tacr1 cre mice support the conclusion that activation of RVM Tacr1 expressing neurons inhibits pruritogen evoked scratching behavior.

RVM Tacr1 expressing neurons inhibit chronic itch

Since activation of RVM Tacr1-expressing neurons inhibited acute pruritogen-evoked scratching behavior, we next wanted to determine whether chronic itch related behaviors would be affected. We used the imiquimod model of psoriasisiform dermatitis in Tacr1 cre mice receiving intra-RVM injection of hM3Dq or control vector. Mice were treated daily with topical application of 5% imiquimod cream for 5 days. This resulted in a significant increase in spontaneous scratching on treatment day 3 (Fig. 4A, dark blue) and significantly increased alloknesis scores on treatment days 1, 3 and 5 (Fig. 4D, dark blue). Application of vehicle (Vanicream) had no effect on spontaneous scratching or alloknesis (Follansbee et al., 2019). Following administration of clozapine on day 5, there was a significant reduction in the number of spontaneous scratch bouts (Fig. 4A, light blue). Fig. 4B shows that scratch bouts in individual animals were significantly reduced after the administration of clozapine. Clozapine administered on days 3 and 5 also significantly reduced alloknesis scores (Fig. 4D, light blue). Fig. 5E shows significant reductions in alloknesis scores of individual animals after as compared to before clozapine. Mice that received intra-RVM microinjection of control vector also showed significant increases in spontaneous scratching (Fig. 4A, dark green) and alloknesis scores (Fig. 4D, dark green) following imiquimod treatment. Administration of clozapine did not significantly

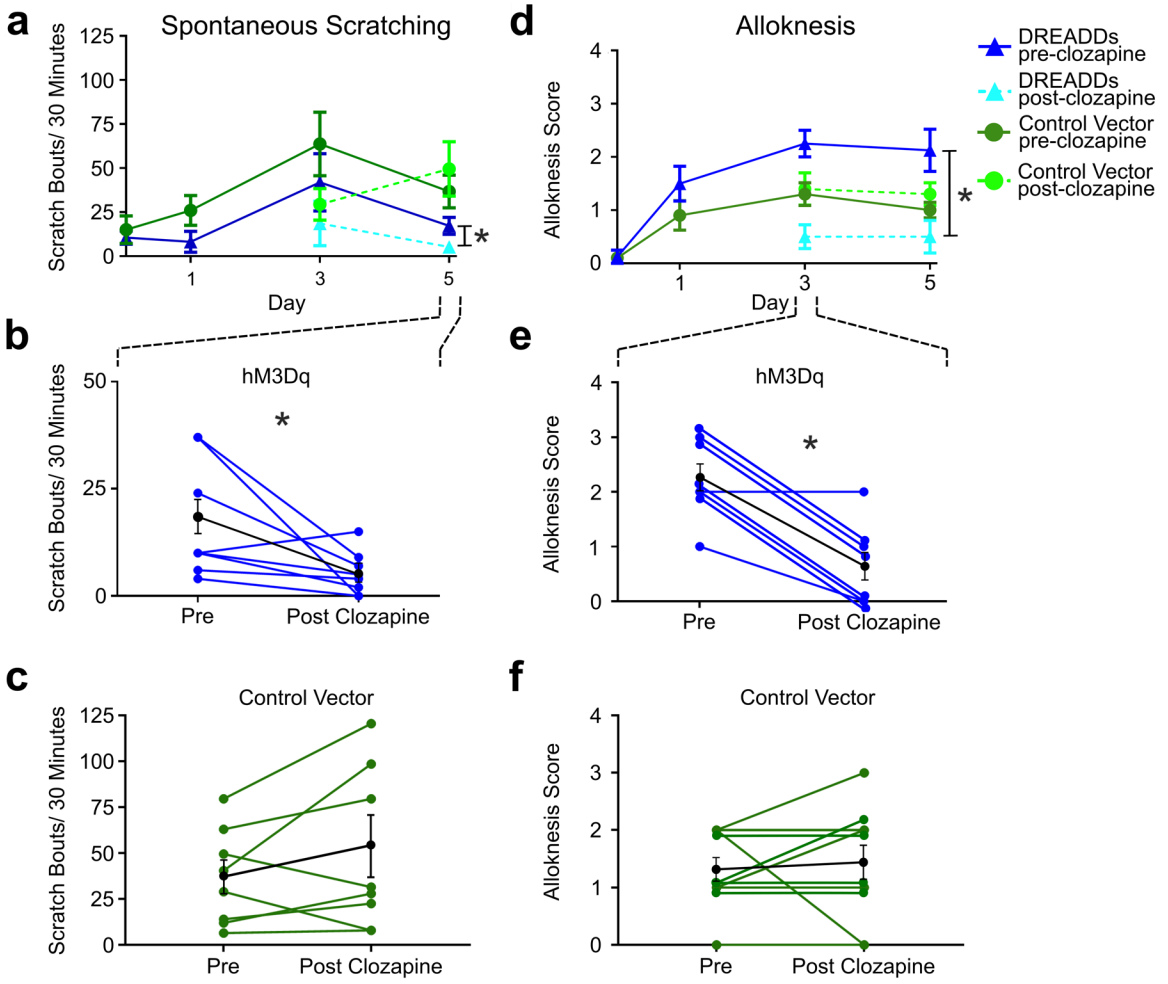

Figure 4: Chemogenetic activation of RVM Tacr1 neurons reduces spontaneous scratching and alloknesis in the imiquimod model of chronic psoriasisiform itch. (A) Application of imiquimod (1%, 0.05 g, Taro) once per day produced a significant increase in spontaneous scratching at day 3 for both DREADDs (dark blue) and control vector (dark green) mice (n = 4 males, 4 females/group). Following clozapine, there was a significant reduction in spontaneous scratching on day 5 for the DREADDs mice (dashed light blue) but no significant change in control vector mice (dashed light green). (B) Graph shows individual DREADDs animals' spontaneous scratch bouts pre- and post-clozapine. Following clozapine there was a significant reduction in scratching. Blue: individual counts; red: mean +/- SEM. (C) Graph as in B for mice in vector control group, in which clozapine had no significant effect. Green: individual counts; red: mean +/- SEM. (D) Imiquimod induced significant increases in alloknesis scores on day 1, 3 and 5 of treatment in DREADDs (dark blue) and vector control (dark green) mice. Following clozapine administration on days 3 and 5 there were significant reductions in alloknesis scores for the DREADDs mice (dashed light blue) but not control vector groups (dashed light green). (E) Clozapine resulted in a significant reduction in alloknesis scores (format as in B). (F) Clozapine had no effect on alloknesis scores in vector controls (format as in C). *p < 0.05, **p < 0.01, ***p < 0.001.

171 affect spontaneous scratching (Fig. 5C) or alloknesis scores (Fig. 5F) in these mice. These

172 results show that activation of RVM Tacr1-expressing neurons reduces itch related behaviors in

a model of chronic itch in addition to acute pruritogen-evoked scratch bouts.

RVM ON cells express Tacr1

Previous reports had shown, in rats, that RVM ON cells were facilitated by local microinjection of SP (Budai et al., 2007; Zhang & Hammond, 2009) and ablation of RVM neurons which express Tacr1, was antihyperalgesic (Khasabov et al., 2017), consistent with a pronociceptive role for RVM ON cells.

We used Tacr1 cre mice which were injected with an AAV encoding channelrhodopsin (AAV5:DIO-ChR2-eYFP). Four weeks later, the mice were anesthetized with sodium pentobarbital for single-unit recording with a microelectrode whose tip extended a few hundred micrometers beyond the tip of an optic fiber it was affixed to (Fig. 5A). Injected mice exhibited robust expression of eYFP in the RVM (Fig. 5B). ON and OFF cells were identified based on their response to a pinch stimulus. Once identified, blue light (473 nm, 0.25-5 mW) was applied and the cell was tested for entrainment to the light stimulus. Fig. 5C shows an example of an ON cell in RVM that responded to pinch prior to the onset of EMG activity and was faithfully entrained to 10 hz light stimulation (Fig. 5D). This neuron received a total of 37 light pulses at 2 hz and fired 32 action potentials within 20 ms of the light onset (Fig. 5E) with a calculated efficiency index of 0.86 (see below), and an average latency of 8.14 ms. The latencies measured presently compare favorably with those reported previously for hippocampal neurons (Zhang et al., 2013). The latency, or on rate, of neuronal activation differs by cell type (Herman et al., 2014) and increases with diminishing light density (Lin et al., 2009). Out of 22 identified ON cells, 17 were entrained to the light stimulus, 1 was inhibited and 4 were not affected (Fig. 6F). It is possible that our estimate is an under representation since viral transduction was not completely efficacious. Since the majority of RVM ON cells were entrained to light stimulation, we conclude that the majority of ON cells likewise express Tacr1.

While our primary interest was RVM ON cells, we wanted to determine whether Tacr1 is also expressed in other cell types, such as RVM OFF cells. During our recordings we often found RVM OFF cells. Out of 14 identified OFF cells, none were directly activated by the light stimulus, with 7 showing a clear inhibitory response to the light stimulation while the other 7 were unaffected (Fig. 5F). Often the degree of inhibition of the OFF cell increased proportionately to the stimulation frequency (Fig. 5G-I). These results support the hypothesis that RVM ON cells provide an inhibitory input onto RVM OFF cells (Fields & Heinricher, 1989) and may underlie the RVM OFF cell mediated pause during noxious stimulation.

Occasionally Neutral cells were identified by their response to optic stimulation (n = 3), and each was strongly entrained (Fig. 5F). Since Neutral cells are numerous, not affected by noxious stimulation and their contribution, if any, to descending modulation is unknown, they were not investigated further. We thus conclude that while most presently-recorded light-sensitive cells were ON cells, other cell types including Neutral cells also expresses Tacr1.

To validate our results from optotagging, we used several metrics to determine whether a light-sensitive neuron was truly entrained to the optic stimulus. We assumed that each optic stimulus was likely to directly excite a neuron expressing ChR2 and tested this in different ways. An efficiency index was calculated to determine whether a neuron was entrained to the optic stimulus, by counting the number of evoked action potentials divided by the number of optic stimuli (Supplemental Fig. 3). The 3 Neutral cells had the highest efficiency index (>1), which was due to occasional firing of “doublet” action potentials in response to the optic stimulus (Supplemental Fig. 3C,D). ON cells classified as light sensitive also had a high efficiency index, which decreased with increasing optic stimulation frequency most likely due to desensitization of ChR2. We additionally assumed that the neuronal firing rate would reflect the number of optic stimuli. Indeed, the neuronal firing rate in light sensitive neurons increased with the stimulation frequency, while non-light sensitive neurons showed no change (Supplemental Fig. 4). In

222 neurons which were inhibited by optic stimulation, there was a decrease in firing rate following

223 light stimulation (Supplemental Fig. 4, OFF cells). Finally, we assumed that the light-evoked

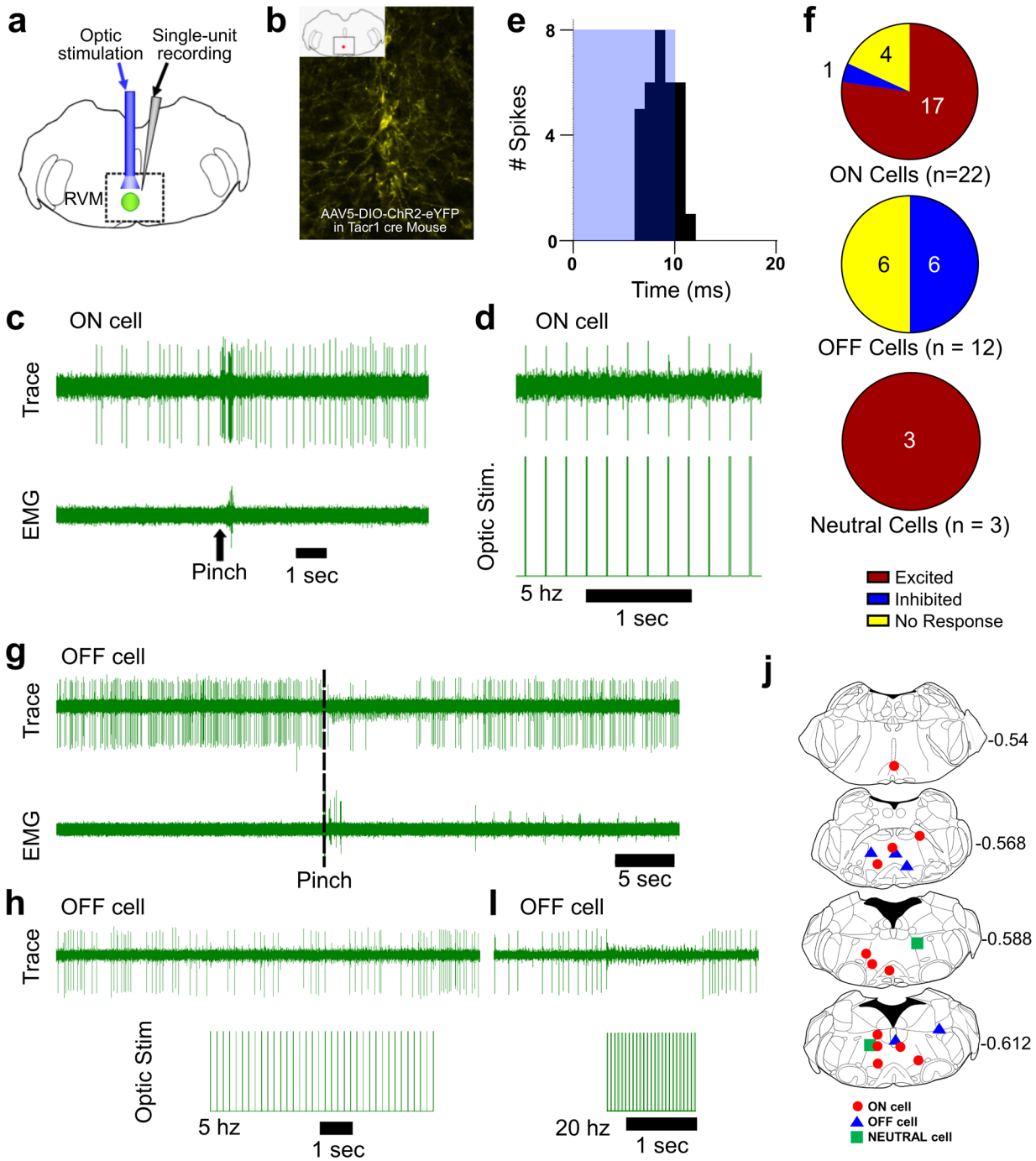

Figure 5: Optotagging of RVM Tacr1 neurons. (A) RVM cells were recorded with a microelectrode coupled to an optic fiber. (B) Injection of AAV-ChR2-eYFP in the RVM of Tacr1 cre$^{+/-}$ mice caused strong expression of eYFP. (C) ON cells were identified based on their pinch-evoked response that preceded the hindlimb withdrawal as monitored by EMG in biceps femoris. (D) Cells identified as RVM ON cells were optically stimulated (5 mW, 472nm). This neuron faithfully responded to each pulse in a 5 hz train. (E) Light entrainment was analyzed by creating peristimulus-time histograms of action potentials that occurred within a 20 msec window following the onset of each light pulse. This neuron responded consistently at a latency of approximately 8.14 msec with a calculated efficiency index of 0.86. (F) Distribution of RVM ON, OFF and Neutral cells which were excited (red), inhibited (blue), or not affected (yellow) by optic stimulation. (G) Application of a pinch stimulus elicited a hindlimb withdrawal (dotted line) and a pause in firing that is typical of OFF cells. (H) There was an intermittent decrease in OFF cell firing during 5 hz optic stimulation and a (I) total cessation of firing during 20 hz optic stimulation. (J) Lesion sites from the optotagging recordings of RVM ON (red circles), OFF (blue triangles) and NEUTRAL cells (green squares). Numbers to right indicate Bregma coordinates.

latency of neuronal action potentials would be consistent. For the population of light-sensitive ON cells, the average latency of responses to the optic stimuli delivered at 2 hz was 7.6 (+/- 1.12) ms (Supplemental Fig. 5). Thus, these experiments strongly support the hypothesis that the majority of RVM ON cells express Tacr1.

Discussion

Previous studies indicate a pronociceptive role for SP acting at Tacr1 expressing neurons in RVM (Budai et al., 2007), many of which have descending spinal projections (Pinto et al., 2008). A novel finding of the present study is that pharmacological and chemogenetic activation of Tacr1-expressing RVM neurons inhibited itch-related scratching behavior, with mild mechanical sensitization and no effect on thermal nociception. Our optotagging experiments provide evidence that the majority of ON cells express Tacr1. These results argue for a causal role of a subpopulation of Tacr1-expressing ON cells in the inhibition of itch-related scratching behavior, in contrast to their pronociceptive role.

Role of SP in RVM in descending modulation of pain and itch

SP (Ljungdahl et al., 1978) and Tacr1 (Saffroy et al., 2003) are present within the RVM. SP acting in the RVM potentiated ON cells, induced pronociceptive behavioral effects and sensitized spinal wide dynamic range dorsal horn neurons (Budai et al., 2007; Khasabov et al.,

2017). SP appears not to be released in the RVM in the absence of injury, but is released under inflammatory conditions elicited by CFA or capsaicin to induce Tacr1-dependent hyperalgesia (Brink et al., 2012; Hamity et al., 2010; Khasabov et al., 2017). The present study expands on this work in important ways. Firstly, we confirm that SP potentiates noxious pinch-evoked responses of mouse RVM ON cells. Secondly, our optotagging data provide evidence that the Tacr1-expressing neurons are ON cells. Importantly, our results support a role for these neurons in descending inhibition of acute and chronic itch. Intra-RVM microinjection of SP or chemogenetic activation of Tacr1-expressing neurons in two different Tacr1 cre lines significantly decreased pruritogen-evoked as well as chronic itch related scratching behavior, while facilitating mechanical nociception in most experiments with no effect on thermal nociception. This latter observation contrasts with a previous report that intra-RVM microinjection of a SP agonist enhanced thermal nociceptive behavior in rats(Khasabov et al., 2017) a discrepancy that might be attributed to a species difference.

Descending Modulation of Itch

Optogenetic activation of GABAergic neurons in RVM facilitated mechanical, but not thermal nociception in mice (François et al., 2017), consistent with our data. The latter authors suggested that the GABAergic RVM neurons might represent ON cells, which descend to presynaptically inhibit mechanonociceptor input onto spinal inhibitory enkephalinergic interneurons that in turn contact the spinal mechanonociceptive pathway. Thus, activation of the descending GABAergic neurons would facilitate mechanical nociception via disinhibition.

Our study shows that RVM Tacr1 neurons represent a population of RVM ON cells, which when activated, reduce pruritogen-evoked scratching. A limitation of this study is that we were not able to directly demonstrate that inhibition of spinal pruriceptive transmission caused the reduction in scratching behavior. Previous studies have shown that 31% of functionally identified RVM ON cells (Vanegas et al., 1984), and 42.5% of Tacr1-expressing RVM neurons (Pinto et

al., 2008), project to the spinal cord, supporting the descending modulation of spinal itch processing. Moreover, recent studies report that activation of spinal projection neurons originating in the locus coeruleus (Koga et al., 2020) or somatosensory cortex (Wu et al., 2021) suppress itch-related scratching behavior. Given this and the historical evidence of the spinal action of RVM ON cells, the most parsimonious explanation is that RVM Tacr1-expressing neurons with descending axons exert an inhibitory effect on spinal pruriceptive transmission to reduce scratching behavior. However, we cannot exclude the possibility that Tacr1-expressing RVM neurons lacking spinal projections exert an antipruritic effect via an unknown supraspinal action.

It was recently reported that activation of neurons in RVM that express the G-protein-coupled estrogen receptor (GPER) suppresses signs of acute and chronic itch (Gao et al., 2021). It is currently not known if GPER-expressing neurons co-express Tacr1.

Electrical stimulation of the PAG inhibited nocifensive behavior in rats (Mayer et al., 1971; Reynolds, 1969), and the PAG projects directly to the RVM (Behbehani & Fields, 1979). Activation of PAG GABAergic neurons, and inhibition of glutamatergic neurons, reduced scratching behavior under both acute and chronic itch conditions (Samineni et al., 2019) but facilitated nocifensive behaviors (Samineni et al., 2017). Activation of Tac1 (SP-expressing) neurons in the PAG was shown to facilitate pruritogen-evoked scratching via release of glutamate onto neurons in the RVM (Gao et al., 2019). In contrast, our results indicate that activation of RVM Tacr1 neurons inhibited pruritogen-evoked scratching behavior. This potentially represents a difference in the synaptic connections of PAG Tac1-expressing neurons with glutamate- and/or Tacr1-expressing RVM neurons. Previous studies have reported projections to RVM from SP-expressing neurons located in dorsolateral PAG, dorsal raphe nucleus, cuneiform nucleus, and lateral hypothalamus (Chen et al., 2013; Holden & Pizzi, 2008; Yin et al., 2014). It is thus possible that Tacr1-expressing RVM neurons that inhibit scratching

291 are activated by different SP inputs than the RVM neurons activated by PAG TAc1-expressing
292 neurons that facilitate scratching.

293 **Modality specific role of RVM ON cells**

294 For decades, the role of RVM ON cells has been considered faciliatory for spinal nociceptive
295 transmission. Our results suggest that the role of RVM ON cells is modality specific, with RVM
296 ON cells facilitating spinal nociceptive while inhibiting pruriceptive transmission. Pruritogens
297 and algogens similarly excited RVM ON and inhibited OFF cells, implying that the opposing
298 modulatory effects of ON cells on spinal nociceptive vs. pruriceptive transmission likely occurs
299 via separate spinal circuits. RVM ON cells have a GABA-mediated inhibitory connection to
300 spinal enkephalinergic neurons (François et al., 2017), raising the possibility that spinal
301 enkephalinergic tone accounts for the opposing effects on spinal nociceptive and pruriceptive
302 transmission. Since pain suppresses itch, we cannot exclude the possibility that activation of
303 spinal pronociceptive circuitry inhibits itch transmission.

304 **Treatment of chronic itch with Tacr1 antagonists**

305 The Tacr1 antagonists aprepitant and serlopitant were recently shown to be partially effective in
306 reducing chronic itch of various etiologies. Tacr1 antagonists might act at Tacr1 that is
307 expressed by spinothalamic and spinoparabrachial neurons (Todd, 2010) to reduce pruriceptive
308 transmission. Indeed, ablation of Tacr1-expressing spinal and medullary neurons reduces
309 pruritogen-evoked scratching behavior (Carstens et al., 2010). The present results suggest that
310 Tacr1 antagonists also have an opposite effect to block Tacr1-mediated descending inhibition of
311 itch. Systemic administration of Tacr1 antagonists thus appear to have offsetting supraspinal
312 and spinal effects, potentially explaining the limited efficacy of Tacr1 antagonists for chronic itch.

313 **Methods**

314 Key Resource Table

Reagent type (species) or resource	Designation	Source or reference	Identifiers
Tacr1 cre Mice/ c57 Background	Tacr1 cre	Dong Lab	
AAV hM3Dq	aav-hSyn-DIO-hM3Dq-mCherry	Addgene	44361-AAV5
AAV mCherry	aav-hSyn-DIO-mCherry	Addgene	50459-AAV5
AAV ChR2	aav-Ef1a-hChR2-mCherry	Addgene	20297-AAV5
Alexa 488 Secondary	Alexa Flour 488	Addgene	ab150077
anti Tacr1	Tacr1 antibody	SCBT	sc-365091 AF488
anti cfos	cfos antibody	Abcam	ab190289
DAPI	DAPI probe	ACD	320858
Substance P	Substance P (SP)	Tocris	1156/5
Histamine Dihydrochloride	Histamine (HA)	Sigma-Aldrich	H7250
Chloroquine Diphosphate	Chloroquine (CLQ)	Sigma-Aldrich	C6628
Pentobarbital Sodium	Pentobarbital	Sigma-Aldrich	P3761
Buprenorphine Hydrochloride	Bup	Amerisoucebergen	NDC42023-179-05
Prism 5	5 Prism	Graphpad	

Animals

Experiments were performed used wild type mice (c57BL/6j, Jackson Labs, Bar Harbor ME), Tacr1 cre$^{+/-}$ (courtesy of Dr. X. Dong, Johns Hopkins University), and Tacr1 cre $^{+/-}$ mice (Huang et al., 2016) of both sexes, 8-10 weeks of age, all on a C57Bl6 background. Mice were given free access to food and water and housed under standard laboratory conditions. Mice were housed in-lab and at the animal housing facility, with a natural light cycle and 12-hour light dark cycle respectively. Mice were allowed to habituate for at least 3 days following transfer from the animal facility to lab housing before use in behavioral experiments. Mice were cohoused with between 1-4 mice/cage. All procedures were approved by the University of California, Davis and University of Pittsburgh Animal Care and Use Committees and followed the ARRIVE guidelines to the extent possible.

Pharmacologic agents

Clozapine was dissolved in saline and administered intraperitoneally (ip) at concentrations of 0.01 and 0.1 mg/kg. Clozapine-N-oxide (CNO;Tocris, Bristol UK) was dissolved in phosphate-buffered saline and administered ip (5 mg/kg). In clozapine and CNO treated mice, experiments were conducted 30 minutes following their administration. Histamine HCl (Sigma, St. Louis MO; 0.5% in 10 µl) or chloroquine diphosphate salt (Sigma; 1% in 10 µl) were dissolved in physiological saline and administered intradermally via a 30 g needle in the nape of the neck. Imiquimod cream (5%; Aldara, 50 mg; 3 M Health Care Limited, UK) was administered topically once per day to shaved skin on the rostral back for 5 days.

Stereotaxic injections and cannula implantation

Animals were anesthetized with 2% isoflurane and placed in a stereotaxic head frame. A burr hole was made in the calvarium and a Hamilton microsyringe loaded with virus was stereotaxically placed such that the tip was at the injection site in RVM (RC: -5.5 to -5.8 mm, ML: 0.0, DV: -4.2 to -6 mm). Virus (0.25-1 µl) containing either AAV5: hSyn-DIO-hM3Dq-mCherry (excitatory DREADD; Addgene, Watertown MA), AAV5: hSyn-DIO-mCherry (control vector, Addgene), or AAV5: hSyn-DIO-ChR2-eYFP (Addgene) was injected into the RVM. Virus was infused at an approximate rate of 100 nL/min. The injection needle was left in place for an additional 15 min post-injection and then slowly withdrawn. The incision was closed using Vetbond and animals were given ketofen (10 mg/kg ip) or buprenorphine (0.05 mg/kg ip) and allowed to recover on a heating pad. A 4 week recovery period ensured prior to experimentation.

For intracranial drug injections, an injection cannula (Plastics One, Roanoke VA) was implanted stereotaxically with the tip targeted 1-2 mm above the RVM. For optogenetic stimulation, following microinjection of AAV5: hSyn-DIO-ChR2-eYFP into RVM, an optic fiber (Doric Lenses,

Quebec Canada) was stereotaxically implanted at the target site. Dental cement was used to affix the injection cannula or optic fiber to the skull. Post-implantation mice received buprenorphine (0.05 mg/kg ip). Mice recovered for at least 4 weeks prior to experimentation.

Intracranial Drug Microinjection

Mice were habituated for 15 minutes prior to intracranial drug injection in clear cylindrical glass enclosures and videotaped from above. Saline (0.5 µl) or Substance P (SP, 0.5 µl, 10 nmol, Tocris, Minneapolis MN) was microinjected. Fifteen minutes post-injection mice were tested for itch or pain behaviors as described below. Both male and female mice were used.

Chemogenetics

Thirty minutes after ip administration of saline, clozapine or CNO, behavioral testing commenced.

Behavior

Scratching behavior: Scratch bouts were defined as back-and-forth hindpaw movements directed to the rostral back, followed by biting the toes and/or placement of the hindpaw on the floor. Scratch bouts elicited by histamine, chloroquine or saline vehicle were videotaped and counts made by at least two blinded observers. Nociceptive behavioral assays (von Frey; Hargreaves) were conducted by investigators blinded as to treatment. Successive behavioral tests were conducted in pseudorandom order and spaced 1 week apart.

Von Frey: Mechanical sensitivity was measured in two ways. Mice stood on a mesh floor allowing access to the plantar surface from below. Using the Chaplan up-down method (Chaplan et al., 1994). calibrated von Frey filaments (North Coast Medical Inc.) were applied to the plantar surface. Paw lifting, shaking, and licking were scored as positive responses. Averaged responses were obtained from each hindpaw, with 3 min between trials on opposite

paws, and 5 min between trials on the same paw. Alternatively, the force at the moment of hindpaw withdrawal was measured using an electronic von Frey device (2390; IITC, Woodland Hills CA). Measurements were again taken from each hindpaw with 3 and 5 min between trials on the same or opposite paw.

Hargreaves: Animals were acclimated on a glass plate held at 30°C (Model 390 Series 8, IITC Life Science Inc.). A radiant heat source was applied to the hindpaw and latency to paw withdrawal was recorded (Hargreaves et al., 1988). Two trials were conducted on each paw, with at least 5 min between tests of opposite paws and at least 10 min between tests of the same paw. To avoid tissue damage, a cut off latency of 20 sec was set. Values from both paws were averaged.

In vivo single-unit recording

Adult mice (6 wk) mice were anesthetized with pentobarbital sodium (60 mg/kg, ip). The head was secured in a stereotaxic frame and an opening was made in the occipital bone. The animal's body temperature was maintained with a heating pad and external heating source. Teflon coated silver wires were inserted into the biceps femoris to record electromyographic (EMG) activity. A single-unit recording microelectrode (10 MOhm, Frederick Haer Inc., Bowdoin ME) was coupled to a 33-gauge injection cannula such that the tip of the recording microelectrode extended several μm beyond the tip of the injection cannula and was inserted into the RVM. ON cells were identified by a hindpaw pinch-evoked increase in firing that preceded the hindlimb withdraw reflex measured as EMG activity from fine wires inserted in the biceps femoris. Once an ON cell was identified, either saline or SP (0.5 μl, 10 nmol) was microinjected and changes in firing rate to repeated consistent pinch stimuli were recorded. Responses to pinch stimuli were normalized to the initial response for each unit. Electrode voltages were amplified and digitized (CED 1401, CED, Cambridge UK) and analyzed with Spike2 (CED). At the end of the recording, a lesion was produced at the last recording site by

399 passing direct current through the microelectrode, the brain was harvested postmortem and
400 postfixed in 10% formalin.

401 Optotagging

402 At least 4 weeks following injection of AAV5: hSyn-DIO-ChR2-eYFP into RVM, single-unit
403 recordings were made from RVM as described above using a Tungsten microelectrode attached
404 to an optic fiber such that the microelectrode tip extended a few hundred microns beyond the
405 optic fiber. In most experiments ON cells were functionally characterized as described above,
406 and OFF cells were characterized by a pinch-evoked pause in ongoing activity that preceded
407 the withdrawal reflex. ON and OFF cells were then tested for entrainment to optic stimulation at
408 473 nm wavelength and 0.25 mW - 5 mW light output (5-20 Hz, 10ms pulse duration) from a
409 laser (Laserglow R471003GX). In some experiments, optic stimulation was used as to isolate
410 light-sensitive neurons, which were then identified as ON, OFF or Neutral based on their
411 response to pinch. Efficiency indices were calculated as the number of action potentials firing
412 within a 20 ms window following the onset of the optic stimulus divided by the total number of
413 optic stimulus pulses, and were used to determine whether a neuron was entrained to the optic
414 stimulus. Both male and female mice were used for all electrophysiological experiments.

415 Imiquimod Treatment

416 Imiquimod cream was applied topically to the shaved area on the rostral back once per day for 5
417 consecutive days. Treatment groups consisted of age-matched male and female NK-1-cre mice
418 that had received intra-RVM injection of AAV5: DIO-hM3Dq-mCherry or the control vector
419 AAV5: hSyn-DIO-mCherry. Imiquimod treatment induced signs of skin pathology including skin
420 scaling and erythema. As measures of chronic itch, we assessed spontaneous scratching, and
421 alloknesis, 23 hours following imiquimod treatment. Mice were videotaped and tested between
422 10 AM and 5 PM, with each individual mouse tested at the same time each day. The mice were

habituated to glass cylinders for 3 successive days prior to recording. Animals were videotaped from above for 30 min. Behavioral videos were analyzed by two blinded observers. Only discrete bouts of spontaneous hindlimb scratches directed towards the application site were counted, as described previously (Akiyama et al., 2016) and summed over the 30 min period. Alloknesis was assessed as previously described (Akiyama et al., 2012). The mouse was placed in an enclosed area and a 0.07g von Frey monofilament was applied to the perimeter of the imiquimod application area 5 consecutive times. The alloknesis score consisted of the number of immediately-occurring hindlimb scratch bouts directed to the stimulus site.

Immunofluorescence

Four weeks after intra-RVM injection of AAV5:hSyn-DIO-hM3Dq-mCherry or the control vector (AAV5:hSyn-DIO-mCherry) in Tacr1 cre mice, clozapine (0.01 mg/kg, i.p.) was injected, followed 1 hr later by perfusion (4% paraformaldehyde), harvesting of brains and post-fixation overnight in 4% paraformaldehyde. Brains were sectioned (20 μm) on a freezing microtome and stained as free floating sections. DREADDs-expressing neurons were counterstained for Tacr1 expression with a conjugated Tacr1 antibody (D-11, sc-365091, Santa Cruz Biotechnology, Dallas TX) at 1:50 overnight at 4°C. c-fos was stained with a primary c-fos antibody (ab190289, Abcam, Cambridge UK) at 1:10,000 overnight at room temperature. Alexa Fluor 488 (ab15077, Abcam) was applied at 1:2000 for 2 hours at room temperature. All slides were mounted with vectashield and imaged with confocal microscopy. Staining intensity was measured relative to the red fluorescence (from DREADDs) and was quantified using FIJI (Schindelin et al., 2012).

Statistical analysis

All statistical analyses were performed using GraphPad Prism. Values are presented as mean +/- SEM. Statistical significance was assessed using students t-test or a two-way, repeated measures ANOVA with Bonferroni's correction, unless otherwise specified. Significance was

447 indicated by $p < 0.05$. Sample sizes were based on pilot data and are similar to those typically
448 used in the field.

449 For analysis of effects of intracranial microinjections, a paired students t-test was used to
450 compare the effects of intracranial injection of saline versus SP on behavioral measures. Two-
451 way ANOVA determined a lack of significant sex x SP microinjection interaction, so the data
452 from both sexes were pooled. For chemogenetic experiments, a paired t-test was used to
453 compare scratch counts and nociceptive measures following vehicle vs. clozapine or CNO
454 injection, or between vector controls and DREADDs mice following clozapine or CNO. For
455 optogenetic experiments a paired t-test was similarly used to compare behavioral measures
456 during and in the absence of optic stimulation.

457 For experiments with imiquimod, paired students t-tests compared the effects of ip injection of
458 saline versus clozapine on spontaneous scratch bouts and alloknesis scores. A two-way
459 ANOVA revealed no interaction for sex x clozapine administration, so the data were pooled for
460 further analysis.

461 For single-unit recordings, a 2-way repeated measures ANOVA with bonferroni post-hoc test
462 was used to compare the neuronal responses to pinch following intra-RVM injection of saline or
463 SP for 60 minutes post-injection.

464 For immunohistochemical staining for c-fos, students t-test compared the staining intensity of c-
465 fos and the proportion of c-fos positive neurons in Tacr1-expressing neurons following
466 administration of clozapine, in mice receiving DREADDs or control vector injections.

467

References

Agostinelli, L. J., & Bassuk, A. G. (2021). Novel inhibitory brainstem neurons with selective projections to spinal lamina I reduce both pain and itch. *Journal of Comparative Neurology*, *529*(8), 2125–2137. https://doi.org/10.1002/cne.25076

Akiyama, T., Carstens, M. I., Ikoma, A., Cevikbas, F., Steinhoff, M., & Carstens, E. (2012). Mouse Model of Touch-Evoked Itch (Alloknesis). *Journal of Investigative Dermatology*, *132*(7), 1886–1891. https://doi.org/10.1038/jid.2012.52

Akiyama, T., Ivanov, M., Nagamine, M., Davoodi, A., Carstens, M. I., Ikoma, A., Cevikbas, F., Kempkes, C., Buddenkotte, J., Steinhoff, M., & Carstens, E. (2016). Involvement of TRPV4 in serotonin-evoked scratching. *Journal of Investigative Dermatology*, *136*(1), 154–160. https://doi.org/10.1038/JID.2015.388

Barbaro, N. M., Heinricher, M. M., & Fields, H. L. (1986). Putative pain modulating neurons in the rostral ventral medulla: Reflex-related activity predicts effects of morphine. *Brain Research*, *366*(1–2), 203–210. https://doi.org/10.1016/0006-8993(86)91296-5

Bartels, D. J. P., Van Laarhoven, A. I. M., Van de Kerkhof, P. C. M., & Evers, A. W. M. (2018). Nocebo effects and scratching behaviour on itch. *Acta Dermato-Venereologica*, *98*(10), 943–950. https://doi.org/10.2340/00015555-2979

Behbehani, M. M., & Fields, H. L. (1979). Evidence that an excitatory connection between the periaqueductal gray and nucleus raphe magnus mediates stimulation produced analgesia. *Brain Research*, *170*(1), 85–93. https://doi.org/10.1016/0006-8993(79)90942-9

Brink, T. S., Pacharinsak, C., Khasabov, S. G., Beitz, A. J., & Simone, D. A. (2012). Differential modulation of neurons in the rostral ventromedial medulla by neurokinin-1 receptors. *Journal of Neurophysiology*, *107*(4), 1210–1221. https://doi.org/10.1152/jn.00678.2011

491 Budai, D., Khasabov, S. G., Mantyh, P. W., & Simone, D. A. (2007). NK-1 Receptors Modulate
492 the Excitability of ON Cells in the Rostral Ventromedial Medulla. *J Neurophysiol*, *97*, 1388–
493 1395. https://doi.org/10.1152/jn.00450.2006

494 Butler, R. K., & Finn, D. P. (2009). Stress-induced analgesia. In *Progress in Neurobiology* (Vol.
495 88, Issue 3, pp. 184–202). Pergamon. https://doi.org/10.1016/j.pneurobio.2009.04.003

496 Carstens, E., Carstens, M. I., Simons, C. T., & Jinks, S. L. (2010). Dorsal horn neurons
497 expressing NK-1 receptors mediate scratching in rats. *NeuroReport*, *21*(4), 303–308.
498 https://doi.org/10.1097/WNR.0b013e328337310a

499 Carstens, E., Follansbee, T. L., & Carstens, M. I. (2020). The Challenge of Basic Itch Research.
500 *Acta Dermato Venereologica*, *100: adc00*, 2–9. https://doi.org/10.2340/00015555-3343

501 Carstens, Earl, Iodi Carstens, M., Akiyama, T., Davoodi, A., & Nagamine, M. (2018). Opposing
502 effects of cervical spinal cold block on spinal itch and pain transmission. *Itch*, *3*(3), 1.
503 https://doi.org/10.1097/itx.0000000000000016

504 Chaplan, S. R., Bach, F. W., Pogrel, J. W., Chung, J. M., & Yaksh, T. L. (1994). Quantitative
505 assessment of tactile allodynia in the rat paw. *Journal of Neuroscience Methods*, *53*(1),
506 55–63. https://doi.org/10.1016/0165-0270(94)90144-9

507 Chebbi, R., Boyer, N., Monconduit, L., Artola, A., Luccarini, P., & Dallel, R. (2014). The nucleus
508 raphe magnus OFF-cells are involved in diffuse noxious inhibitory controls. *Experimental*
509 *Neurology*, *256*, 39–45. https://doi.org/10.1016/j.expneurol.2014.03.006

510 Chen, T., Wang, X. L., Qu, J., Wang, W., Zhang, T., Yanagawa, Y., Wu, S. X., & Li, Y. Q.
511 (2013). Neurokinin-1 receptor-expressing neurons that contain serotonin and gamma-
512 aminobutyric acid in the rat rostroventromedial medulla are involved in pain processing.
513 *Journal of Pain*, *14*(8), 778–792. https://doi.org/10.1016/j.jpain.2013.02.002

514 Damien, J., Colloca, L., Bellei-Rodriguez, C. É., & Marchand, S. (2018). Pain Modulation: From
515 Conditioned Pain Modulation to Placebo and Nocebo Effects in Experimental and Clinical
516 Pain. In *International Review of Neurobiology* (Vol. 139, pp. 255–296). Academic Press
517 Inc. https://doi.org/10.1016/bs.irn.2018.07.024

518 Fields, H. L. (2000). Pain modulation: Expectation, opioid analgesia and virtual pain. In *Progress*
519 *in Brain Research* (Vol. 122, pp. 245–253). Elsevier. https://doi.org/10.1016/s0079-
520 6123(08)62143-3

521 Fields, H. L. (2004). State-dependent opioid control of pain. *Nature Reviews Neuroscience*,
522 *5*(7), 565–575. https://doi.org/10.1038/nrn1431

523 Fields, H. L., & Basbaum, A. I. (1978). Brainstem Control of Spinal Pain-Transmission Neurons.
524 *Annual Review of Physiology*, *40*(1), 217–248.
525 https://doi.org/10.1146/annurev.ph.40.030178.001245

526 Fields, H. L., & Heinricher, M. M. (1985). Anatomy and physiology of a nociceptive modulatory
527 system. *Philosophical Transactions of the Royal Society of London. Series B, Biological*
528 *Sciences*, *308*(1136), 361–374. https://doi.org/10.1098/rstb.1985.0037

529 Fields, H. L., & Heinricher, M. M. (1989). Brainstem Modulation of Nociceptor-Driven Withdrawal
530 Reflexes. *Annals of the New York Academy of Sciences*, *563*(1), 34–44.
531 https://doi.org/10.1111/j.1749-6632.1989.tb42188.x

532 Fields, H. L., Vanegas, H., Hentall, I. D., & Zorman, G. (1983). Evidence that disinhibition of
533 brain stem neurones contributes to morphine analgesia. *Nature*, *306*(5944), 684–686.
534 https://doi.org/10.1038/306684a0

535 Follansbee, T., Akiyama, T., Fujii, M., Davoodi, A., Nagamine, M., Iodi Carstens, M., &
536 Carstens, E. (2018). Effects of pruritogens and algogens on rostral ventromedial medullary

537 ON and OFF cells. *Journal of Neurophysiology*, *120*(5), 2156–2163.
538 https://doi.org/10.1152/jn.00208.2018

539 Follansbee, Taylor, Zhou, Y., Wu, X., Delahanty, J., Nguyen, A., Domocos, D., Carstens, M. I.,
540 Hwang, S. T., & Carstens, E. (2019). Signs of chronic itch in the mouse imiquimod model
541 of psoriasiform dermatitis. *Itch*, *4*(3), e25. https://doi.org/10.1097/itx.0000000000000025

542 François, A., Low, S. A., Sypek, E. I., Christensen, A. J., Sotoudeh, C., Beier, K. T.,
543 Ramakrishnan, C., Ritola, K. D., Sharif-Naeini, R., Deisseroth, K., Delp, S. L., Malenka, R.
544 C., Luo, L., Hantman, A. W., & Scherrer, G. (2017). A Brainstem-Spinal Cord Inhibitory
545 Circuit for Mechanical Pain Modulation by GABA and Enkephalins. *Neuron*, *93*(4), 822-
546 839.e6. https://doi.org/10.1016/j.neuron.2017.01.008

547 Gao, T., Dong, L., Qian, J., Ding, X., Zheng, Y., Wu, M., Meng, L., Jiao, Y., Gao, P., Luo, P.,
548 Zhang, G., Wu, C., Shi, X., & Rong, W. (2021). G-Protein-Coupled Estrogen Receptor
549 (GPER) in the Rostral Ventromedial Medulla Is Essential for Mobilizing Descending
550 Inhibition of Itch. *Journal of Neuroscience*, *41*(37), 7727–7741.
551 https://doi.org/10.1523/JNEUROSCI.2592-20.2021

552 Gao, Z. R., Chen, W. Z., Liu, M. Z., Chen, X. J., Wan, L., Zhang, X. Y., Yuan, L., Lin, J. K.,
553 Wang, M., Zhou, L., Xu, X. H., & Sun, Y. G. (2019). Tac1-Expressing Neurons in the
554 Periaqueductal Gray Facilitate the Itch-Scratching Cycle via Descending Regulation.
555 *Neuron*, *101*(1), 45-59.e9. https://doi.org/10.1016/j.neuron.2018.11.010

556 Gomez, J. L., Bonaventura, J., Lesniak, W., Mathews, W. B., Sysa-Shah, P., Rodriguez, L. A.,
557 Ellis, R. J., Richie, C. T., Harvey, B. K., Dannals, R. F., Pomper, M. G., Bonci, A., &
558 Michaelides, M. (2017). Chemogenetics revealed: DREADD occupancy and activation via
559 converted clozapine. *Science*, *357*(6350).
560 http://science.sciencemag.org/content/sci/357/6350/503.full.pdf

561 Hamity, M. V., White, S. R., & Hammond, D. L. (2010). Effects of neurokinin-1 receptor agonism
562 and antagonism in the rostral ventromedial medulla of rats with acute or persistent
563 inflammatory nociception. *Neuroscience*, *165*(3), 902–913.
564 https://doi.org/10.1016/j.neuroscience.2009.10.064

565 Heinricher, M. M., Tavares, I., Leith, J. L., & Lumb, B. M. (2009). Descending control of
566 nociception: Specificity, recruitment and plasticity. In *Brain Research Reviews* (Vol. 60,
567 Issue 1, pp. 214–225). https://doi.org/10.1016/j.brainresrev.2008.12.009

568 Herman, A. M., Huang, L., Murphey, D. K., Garcia, I., & Arenkiel, B. R. (2014). Cell type-specific
569 and time-dependent light exposure contribute to silencing in neurons expressing
570 Channelrhodopsin-2. *ELife*, *3*, 1–18. https://doi.org/10.7554/elife.01481

571 Holden, J. E., & Pizzi, J. A. (2008). Lateral hypothalamic-induced antinociception may be
572 mediated by a substance P connection with the rostral ventromedial medulla. *Brain*
573 *Research*, *1214*, 40–49. https://doi.org/10.1016/j.brainres.2008.03.051

574 Huang, H., Kuzirian, M. S., Cai, X., Snyder, L. M., Cohen, J., Kaplan, D. H., & Ross, S. E.
575 (2016). Generation of a NK1R-CreER knockin mouse strain to study cells involved in
576 Neurokinin 1 Receptor signaling. *Genesis*, *54*(11), 593–601.
577 https://doi.org/10.1002/dvg.22985

578 Jennings, E. M., Okine, B. N., Roche, M., & Finn, D. P. (2014). Stress-induced hyperalgesia. In
579 *Progress in Neurobiology* (Vol. 121, pp. 1–18). Elsevier Ltd.
580 https://doi.org/10.1016/j.pneurobio.2014.06.003

581 Khasabov, S. G., Malecha, P., Noack, J., Tabakov, J., Giesler, G. J., & Simone, D. A. (2017).
582 Hyperalgesia and sensitization of dorsal horn neurons following activation of NK-1
583 receptors in the rostral ventromedial medulla. *Journal of Neurophysiology*, *118*(5), 2727–
584 2744. https://doi.org/10.1152/jn.00478.2017

585 Khasabov, S. G., Wang, J. C., Simone, D. A., & Strichartz, G. R. (2017). A role for neurokinin-1
586 receptor neurons in the rostral ventromedial medulla in the development of chronic
587 postthoracotomy pain. *Pain*, *158*, 1332–1341.

588 Koga, K., Shiraishi, Y., Yamagata, R., Tozaki-Saitoh, H., Shiratori-Hayashi, M., & Tsuda, M.
589 (2020). Intrinsic braking role of descending locus coeruleus noradrenergic neurons in acute
590 and chronic itch in mice. *Molecular Brain*, *13*(1), 1–11.

591 Le Bars, D. (2002). The whole body receptive field of dorsal horn multireceptive neurones. In
592 *Brain Research Reviews* (Vol. 40, Issues 1–3, pp. 29–44). https://doi.org/10.1016/S0165-
593 0173(02)00186-8

594 Lin, J. Y., Lin, M. Z., Steinbach, P., & Tsien, R. Y. (2009). Characterization of engineered
595 channelrhodopsin variants with improved properties and kinetics. *Biophysical Journal*,
596 *96*(5), 1803–1814. https://doi.org/10.1016/j.bpj.2008.11.034

597 Liu, M. Z., Chen, X. J., Liang, T. Y., Li, Q., Wang, M., Zhang, X. Y., Li, Y. Z., Sun, Q., & Sun, Y.
598 G. (2019). Synaptic control of spinal GRPR+ neurons by local and long-range inhibitory
599 inputs. *Proceedings of the National Academy of Sciences of the United States of America*,
600 *116*(52), 27011–27017. https://doi.org/10.1073/pnas.1905658116

601 Ljungdahl, Å., Hökfelt, T., & Nilsson, G. (1978). Distribution of substance P-like
602 immunoreactivity in the central nervous system of the rat-I. Cell bodies and nerve
603 terminals. *Neuroscience*, *3*(10). https://doi.org/10.1016/0306-4522(78)90116-1

604 Lockwood, S., & Dickenson, A. H. (2020). What goes up must come down: insights from studies
605 on descending controls acting on spinal pain processing. In *Journal of Neural Transmission*
606 (Vol. 127, Issue 4, pp. 541–549). Springer. https://doi.org/10.1007/s00702-019-02077-x

607 Mayer, D. J., Wolfle, T. L., Akil, H., Carder, B., & Liebeskind, J. C. (1971). Analgesia from

electrical stimulation in the brainstem of the rat. *Science*, *174*(4016), 1351–1354. https://doi.org/10.1126/science.174.4016.1351

Millan, M. J. (2002). Descending control of pain. In *Progress in Neurobiology* (Vol. 66, Issue 6, pp. 355–474). https://doi.org/10.1016/S0301-0082(02)00009-6

Ossipov, M. H., Morimura, K., & Porreca, F. (2014). Descending pain modulation and chronification of pain. In *Current Opinion in Supportive and Palliative Care* (Vol. 8, Issue 2, pp. 143–151). Lippincott Williams and Wilkins. https://doi.org/10.1097/SPC.0000000000000055

Pinto, M., Sousa, M., Lima, D., & Tavares, I. (2008). Participation of μ-opioid, GABA B , and NK1 receptors of major pain control medullary areas in pathways targeting the rat spinal cord: Implications for descending modulation of nociceptive transmission. *The Journal of Comparative Neurology*, *510*(2), 175–187. https://doi.org/10.1002/cne.21793

Reynolds, D. V. (1969). Surgery in the rat during electrical analgesia induced by focal brain stimulation. *Science*, *164*(3878), 444–445. https://doi.org/10.1126/science.164.3878.444

Saffroy, M., Torrens, Y., Glowinski, J., & Beaujouan, J. C. (2003). Autoradiographic distribution of tachykinin NK2 binding sites in the rat brain: Comparison with NK1 and NK3 binding sites. *Neuroscience*, *116*(3), 761–773. https://doi.org/10.1016/S0306-4522(02)00748-0

Samineni, V. K., Grajales-Reyes, J. G., Copits, B. A., O'Brien, D. E., Trigg, S. L., Gomez, A. M., Bruchas, M. R., & Gereau, R. W. (2017). Divergent modulation of nociception by glutamatergic and GABAergic neuronal subpopulations in the periaqueductal gray. *ENeuro*, *4*(2). https://doi.org/10.1523/ENEURO.0129-16.2017

Samineni, V. K., Grajales-Reyes, J. G., Sundaram, S. S., Yoo, J. J., Gereau, R. W., & Gereau Iv, R. W. (2019). Cell type-specific modulation of sensory and affective components of itch

631 in the periaqueductal gray. *Nature Communications*, *10*(1), 1–15.
632 https://doi.org/10.1038/s41467-019-12316-0

633 Schindelin, J., Arganda-Carreras, I., Frise, E., Kaynig, V., Longair, M., Pietzsch, T., Preibisch,
634 S., Rueden, C., Saalfeld, S., Schmid, B., Tinevez, J. Y., White, D. J., Hartenstein, V.,
635 Eliceiri, K., Tomancak, P., & Cardona, A. (2012). Fiji: An open-source platform for
636 biological-image analysis. In *Nature Methods* (Vol. 9, Issue 7, pp. 676–682).
637 https://doi.org/10.1038/nmeth.2019

638 Todd, A. J. (2010). Neuronal circuitry for pain processing in the dorsal horn. *Nature Reviews*
639 *Neuroscience*, *11*(12), 823–836. https://doi.org/10.1038/nrn2947

640 Vanegas, H., Barbaro, N. M., & Fields, H. L. (1984). Tail-flick related activity in medullospinal
641 neurons. *Brain Research*, *321*(1), 135–141. https://doi.org/10.1016/0006-8993(84)90689-9

642 Wager, T. D., & Atlas, L. Y. (2015). The neuroscience of placebo effects: Connecting context,
643 learning and health. In *Nature Reviews Neuroscience* (Vol. 16, Issue 7, pp. 403–418).
644 Nature Publishing Group. https://doi.org/10.1038/nrn3976

645 Wu, Z. H., Shao, H. Y., Fu, Y. Y., Wu, X. B., Cao, D. L., Yan, S. X., Sha, W. L., Gao, Y. J., &
646 Zhang, Z. J. (2021). Descending Modulation of Spinal Itch Transmission by Primary
647 Somatosensory Cortex. *Neuroscience Bulletin*, *37*(9), 1345–1350.
648 https://doi.org/10.1007/S12264-021-00713-9/FIGURES/2

649 Yin, J.-B., Wu, H.-H., Dong, Y.-L., Zhang, T., Wang, J., Zhang, Y., Wei, Y.-Y., Lu, Y.-C., Wu, S.-
650 X., Wang, W., & Li, Y.-Q. (2014). Neurochemical properties of BDNF-containing neurons
651 projecting to rostral ventromedial medulla in the ventrolateral periaqueductal gray. *Frontiers*
652 *in Neural Circuits*, *8*, 137. https://doi.org/10.3389/fncir.2014.00137

653 Zhang, L., & Hammond, D. L. (2009). Substance P enhances excitatory synaptic transmission

654 on spinally projecting neurons in the rostral ventromedial medulla after inflammatory injury.
655 *Journal of Neurophysiology*, *102*(2), 1139–1151. https://doi.org/10.1152/jn.91337.2008

656 Zhang, S. J., Ye, J., Miao, C., Tsao, A., Cerniauskas, I., Ledergerber, D., Moser, M. B., &
657 Moser, E. I. (2013). Optogenetic dissection of entorhinal-hippocampal functional
658 connectivity. *Science*, *340*(6128), 44. https://doi.org/10.1126/science.1232627

659

660

Acknowledgements: We would like to thank Dr. Dong (Johns Hopkins University) for the generous donation of Tac1r-cre mice.

Author Contributions: T.F., D.D., E.N., A.B., A.N., L.V., M.I.C., and K.T. performed experiments; T.F., M.I.C, E.N., S.R., and E.C. analyzed data; T.F., E.N., S.R., and E.C. edited and revised manuscript; T.F., S.R., and E.C. approved the final version of the manuscript: T.F., E.C. conceived and designed research, T.F. and E.C. interpreted results of experiments; T.F. and E.C. prepared figures; T.F. and E.C. drafted manuscript.

669 **Supplemental Figures**

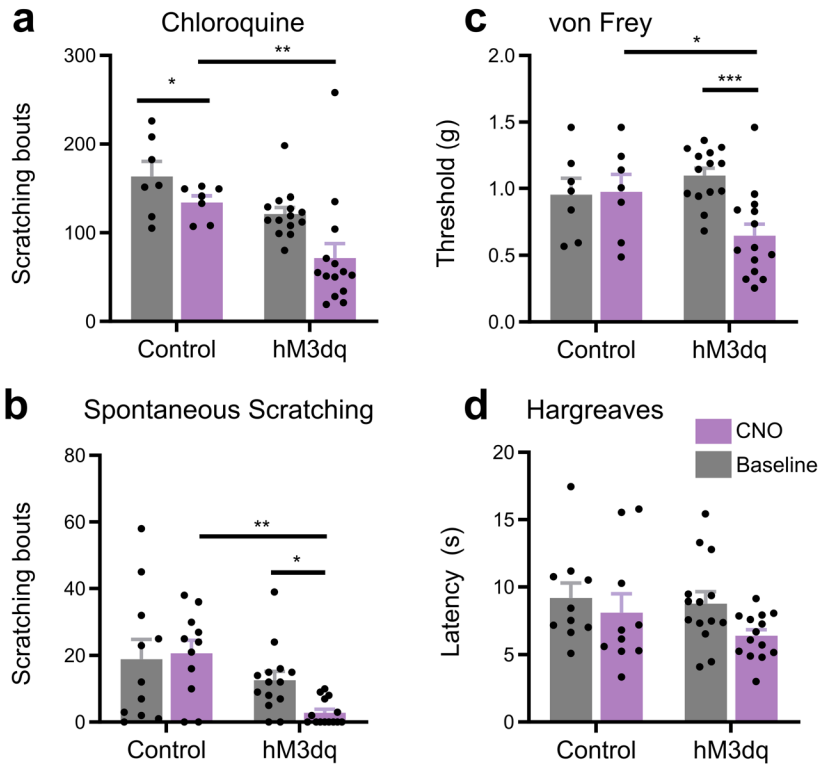

Supplemental Figure 1. Chemogenetic activation of RVM *Tacr1* expressing neurons inhibits itch related behavior. *Tacr1*creER mice were injected with AAV2-DIO-hM3Dq-mCherry. (A) CNO administration significantly reduced chloroquine evoked scratch bouts in DREADDs but not control vector mice (n = 5-7 males, 5-7 females). (B) CNO reduced spontaneous scratching in hM3Dq-expressing but not control vector mice (n = 5 males, 5 females). (C) CNO administration significantly reduced mechanical withdrawal thresholds in DREADDs but not control vector mice (n = 5-7 males, 5-7 females). (D) CNO did not affect thermal withdrawal latency in any group (n = 5-7 males, 5-7 females).

670

671

672

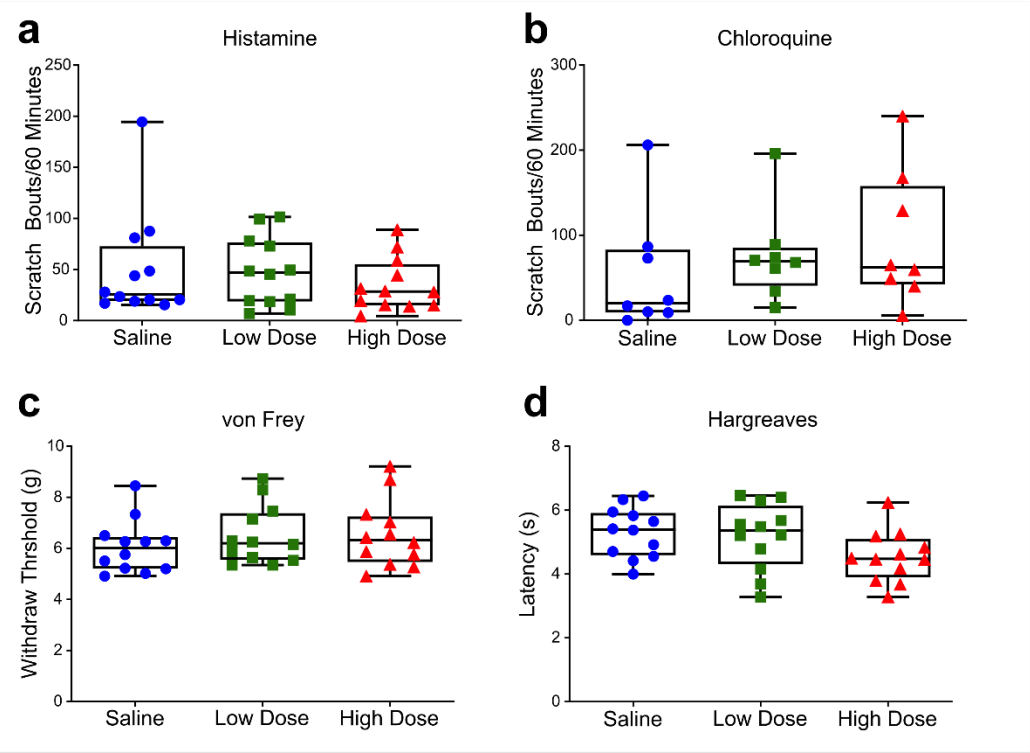

Supplemental Figure 2: Clozapine administration does not affect acute itch or pain behavior. Saline, low dose clozapine (0.01 mg/kg) or high dose clozapine (0.1 mg/kg) was administered systemically, followed by tests for acute itch and pain behaviors. (A, B) Clozapine did not significantly affect the number of scratch bouts elicited by intradermal injection of histamine (A) or chloroquine (B). (C, D) Clozapine also did not significantly affect the respective latency or threshold of hindlimb withdrawals elicited by acute thermal (C) or mechanical (D) stimuli. (A,C and D) n = 6 males, 6 females; (B) n = 5 males, 3 females. P>0.05, 1-way ANOVA followed by Bonferroni post hoc test.

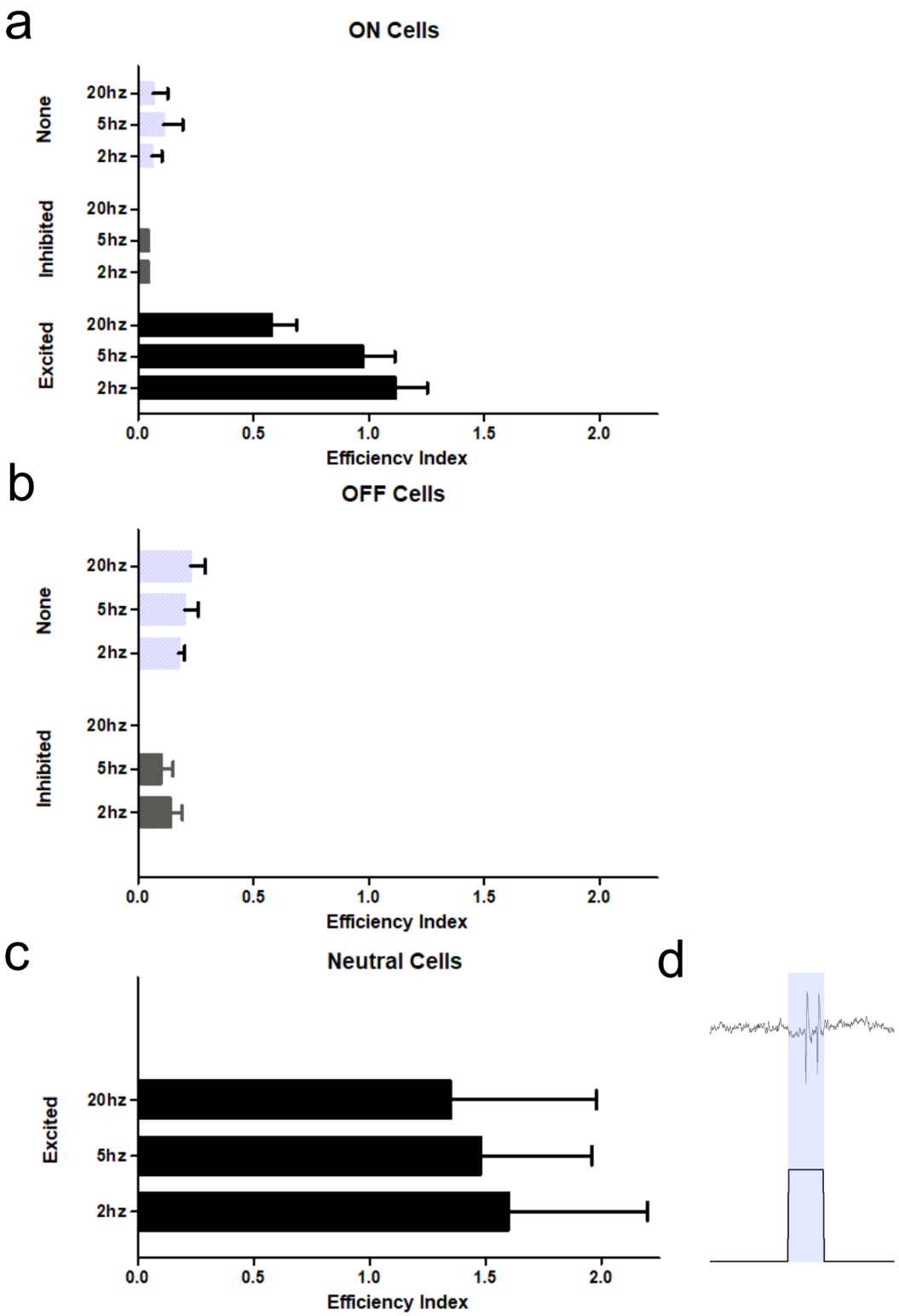

Supplemental Figure 3: Efficiency index of classified RVM neurons. (A-C) Identified ON (A), OFF (B), and NEUTRAL (C) cells were tested for efficiency to respond within 20 msec following the onset of an optic stimulus. Neurons which were excited by optic stimulation had a robust efficiency index (approaching or >1) compared to neurons inhibited or unaffected (none) by optic stimulation. (D) Neutral cell doublet.

673

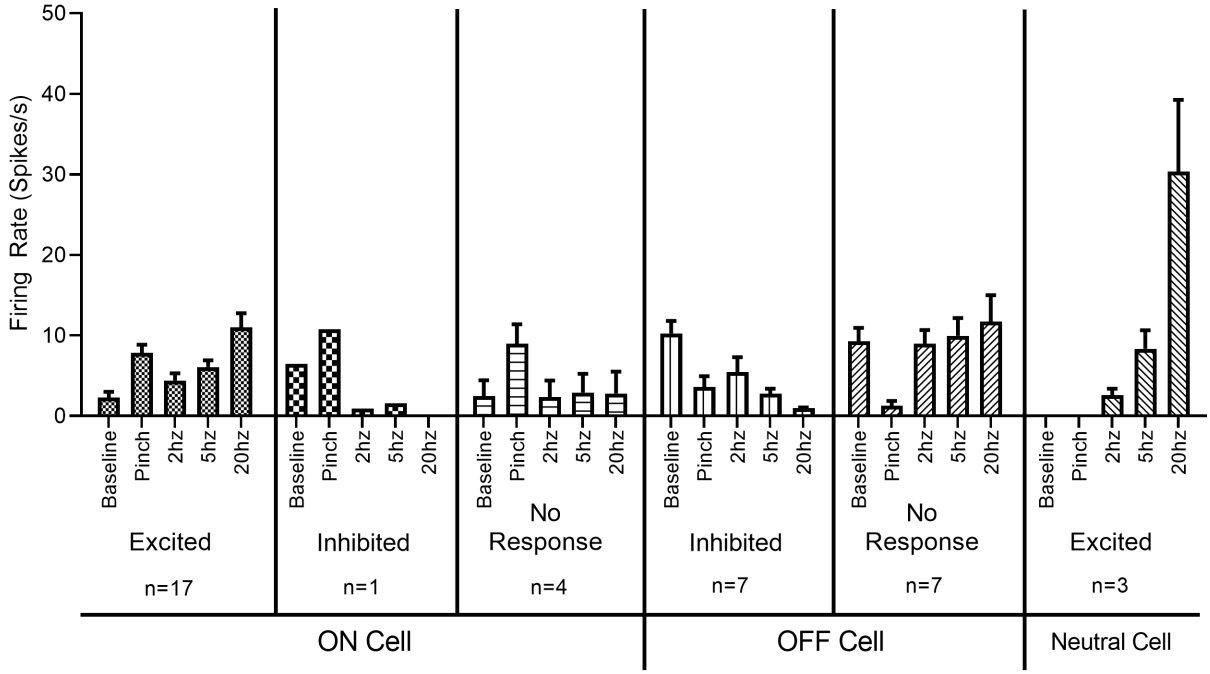

Supplemental Figure 4: Firing rates of classified RVM neurons in response to optic stimulation.

674

675

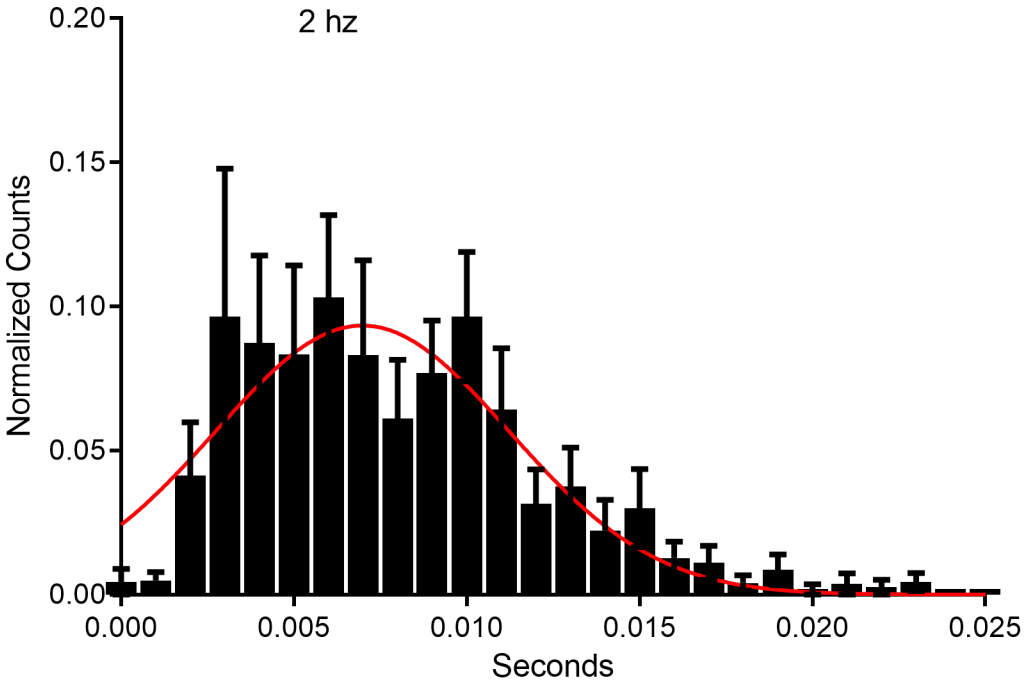

Supplemental Figure 5: Response latency of ON cells to optic stimulation. RVM neurons (n = 17) which responded to optic stimulation at 2 hz, had averaged response latencies of approximately 7.6 +/- 1.12 msec.

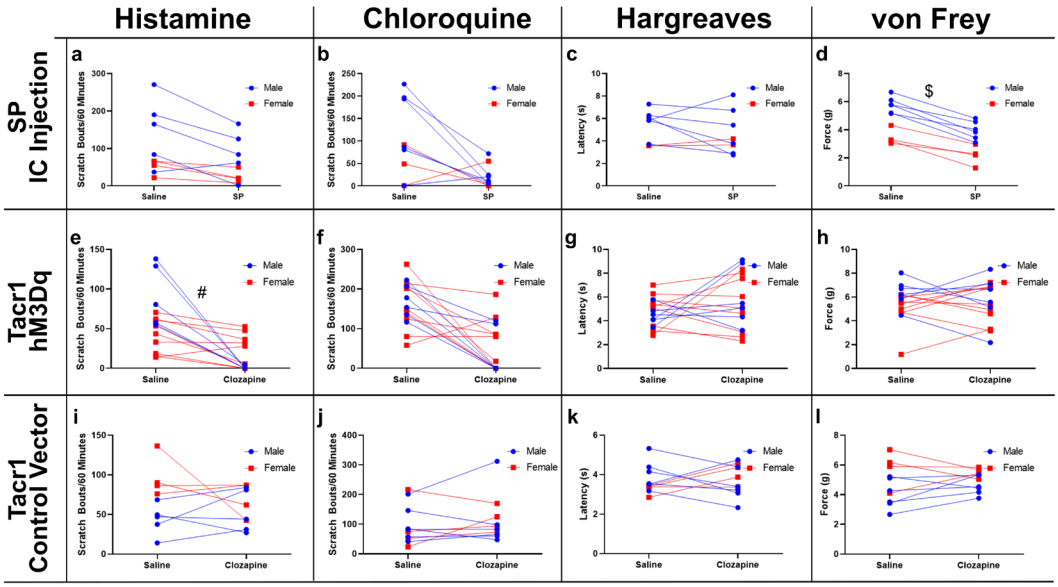

Supplemental Figure 6: Sex differences. Graphs are replotted with data sorted into male (blue) and females (red). (A-C) There were no significant sex differences following intramedullary microinjection of saline or SP for histamine- (A) or chloroquine-evoked scratching (B), or for thermal withdrawal latencies (C). (D) Males exhibited a significantly higher mechanical withdrawal threshold following intramedullary saline ($; $p<0.001$), while both sexes showed a significant reduction in withdrawal threshold following intramedullary SP. (E) Suppression of histamine-evoked scratching following clozapine was significantly greater in males (#; $p<0.01$) . (F-H) There were no sex differences for chloroquine-evoked scratching (F), thermal withdrawal latency (K) or mechanical withdrawal threshold (H). (I-L) There were no sex difference for histamine-(I) or chloroquine- evoked scratch bouts (J), thermal withdrawal latency (K), or mechanical withdrawal threshold (L).

676